CONF-850670--14

DE85 010499

Analysis of Seismic Sloshing of Reactor Tanks Considering Submerged Components and Seismic Isolation

D. C. Ma and Y. W. Chang
Reactor Analysis and Safety Division
Argonne National Laboratory
9700 South Cass Avenue
Argonne, Illinois 60439, U.S.A.

Submitted to
1985 ASME PVP Conference
to be held at
New Orleans, LA
June 23-28, 1985

DISCLAIMER

ABSTRACT

A study of the seismic sloshing response of a large pool-type reactor tank with several deck-mounted components is presented. The main objective of the study is to investigate the effects of internal components on the sloshing response and to determine the sloshing loads on the components. The study shows that the presence of internal components can significantly change the dynamic characteristics of the sloshing motion. The sloshing frequencies of a tank with internal components are considerably higher than those of a tank without internals. The higher sloshing frequencies reduce the sloshing wave height on the free surface but the dynamic pressures of the fluid are increased. The effects of seismic isolation on sloshing response are also presented.

INTRODUCTION

Large-diameter Liquid Metal Fast Breeder Reactor (LMFBR) tanks contain large volume of sodium coolant and many submerged components. A reactor tank of 70 ft in diameter contains 5,000,000 lbs. of sodium coolant. Since most reactor components are submerged in the sodium coolant, the fluid-structure interaction during seismic disturbances plays an important role in the dynamic response of reactor system. This is especially true for those large-size components such as IHXs and pumps which are mounted on the reactor cover head (deck) and submerged into the coolant. The sloshing loads and free-surface wave height are of important concern in the design of those components.

Sloshing behavior of liquid-containers has been studied extensively by analytical methods [1-7] and experimental tests [8-13]. Those studies, however, are limited to the containers which have no internal components. Because they do not consider the existence of internal components, their formulations are rather simple and can be readily applied to reactor tanks. At the present time, the sloshing response of reactor tanks is determined from a simple design procedure as outlined in [4]. Since those methods do not provide calculations for internal components, sloshing loads on internal components are totally ignored in the current design practice. The sloshing waveheight predicted by those methods which consider no internal components can not be used directly to reactor tanks that have many internal components.

This paper presents a method on seismic sloshing analysis of reactor tanks considering the presence of the submerged components. The effects of seismic isolation on sloshing is also described. Since frequencies of coolant sloshing and structural vibrations are well separated, the tank wall and internal components can be assumed to be rigid in the sloshing analysis. For comparison purpose, both cylindrical and rectangular tanks are studied. In the study, the sloshing loads exerted on the components are determined. The effects of the submerged components on sloshing frequencies, wave patterns, and wave height are investigated. The analysis is performed by a finite-element computer program, FLUSTR-ANL developed at Argonne National Laboratory.

Six sections are contained in this paper. The matrix equations of fluid motion based on finite-element spatial discretation and the methodology to treat the free-surface effects are described in Section 2. The sloshing response of the cylindrical and rectangular tanks are presented in Sections 3 and 4, respectively. The effects of seismic isolation on sloshing response is discussed in Section 5. The conclusions are given in Section 6.

EQUATIONS OF MOTION AND TREATMENTS OF FREE-SURFACE EFFECTS

The matrix equations of fluid motion and treatments of free-surface effects are briefly described in this section. For detailed finite-element formulation, interested readers should refer to Refs. 14 and 15. The matrix equations of motion for small-displacement, inviscid fluid under seismic excitation can be expressed as

$$M_f \ddot{d} + K_f d = f \ , \qquad (1)$$

where M_f and K_f are mass and stiffness matrices of fluid, respectively, and f is the external force vector. d is the displacement. A superscript dot designates time (t) derivatives.

If the free-surface wave is small, the wave effects can be represented by the perturbation pressures P_{fs} acting on the normal direction of the undeformed free-surface and included explicitly in Eq. (1) through the external force vector. The perturbation pressure is obtained from

$$P_{fs} = \rho g d_{fs} , \quad (2)$$

where ρ is the mass density of fluid, g is the gravitational acceleration, and d_{fs} is the free-surface displacement in the direction of gravity. Following the standard finite-element method, the perturbation pressures can be assembled to external force vector acting on the free-surface elements.

The free-surface wave effects can also be included implicitly in Eq. (1) through the free-surface spring elements as

$$M_f \ddot{d} + (K_f + K_{fs}) d = f , \quad (3)$$

where K_{fs} is the stiffness of the spring. K_{fs} is determined by

$$K_{fs} = \rho g A_e , \quad (4)$$

in which A_e is the free-surface area of element "e".

The seismic loads can also be included in the external load vector as

$$f = -M_f \ddot{d}_g , \quad (5)$$

in which $\ddot{d}_g$ is the seismic excitation in terms of ground acceleration time history. Equation (1) is integrated by the predictor-corrector integration scheme [14,15]. The fluid dynamic pressure P is obtained from the penalty formulation

$$P = -\lambda d_{i,i} , \quad (6)$$

where λ and $d_{i,i}$ are the penalty parameter and displacement divergence, respectively.

SLOSHING RESPONSE OF REACTOR TANKS WITH INTERNAL COMPONENTS

The sloshing response of reactor tanks with no internal components has been studied by Ma, et al. [16-20]. This section describes a study performed on the sloshing of the reactor tanks with internal components. The finite-element model and dimensions of the tank and components used in the study is shown in Fig. 1, which represents the fluid in the upper part of the commercial-size LMFBR reactor tank that will participate in sloshing. The fluid in the lower part of the tank is completely trapped; it does not participate in sloshing motion and, therefore, is omitted. The component at the center of the tank represents an upper internal structure (UIS); the other six off-center components represent three intermediate heat exchangers (IHXs) and three pumps, which will normally appear in a large pool-type reactor. The tank and components are assumed to be rigid. The fluid is simulated by the displacement-based continuum elements. Only linear sloshing is considered. The free-surface wave effect is treated by the perturbation pressure approach as mentioned in the previous section. The input motion is a 10-s acceleration time history having a maximum acceleration of 1 g. After 10 s, the seismic ground motion is assumed to have terminated. However, analysis of sloshing motion is carried out to 50 s, since sloshing is a long-duration motion. For comparison purpose, a similar analysis is also performed on a reactor tank which has a UIS but no off-center components. The mathematical model of that reactor is shown in Fig. 2.

The computed free-surface wave patterns of these two cases at instant of t = 15 s are shown in Figs. 3 and 4. As can be seen, the sloshing wave height of the tank with UIS only (see Fig. 3) has a $\cos\theta$ distribution in the circumferential direction of the tank. The circumferential wave patterns of the tank with UIS and other components (see Fig. 4) is, however, quite different. It no longer has a distinct $\cos\theta$ distribution in the circumferential direction of the tank. Because of the presence of internal components, the free surface exhibits many peaks, i.e., up-and-down wave patterns when the coolant sloshes. This is clearly demonstrated in Fig. 4. Also, the presence of the internal components, i.e., IHXs and pumps, affects the sloshing frequencies significantly. In the case of no off-center component, the sloshing response is dominated by two sloshing modes, one in the radial direction (antisymmetric) and the other in the tangential direction. The modal shapes of these two modes are shown in Fig. 5 in which H and L indicate the high and low lines of the free-surface, and 0 represents a zero line. The free-surface wave height in the radial antisymmetric mode is primarily caused by fluid flowing in the radial direction of the tank, whereas the wave height in the tangential mode is mainly caused by fluid flowing in the circumferential direction of the tank. The radial antisymmetric mode is the first radial mode which has a sloshing frequency of 0.28 Hz that can be clearly observed from the calculated wave-height time history and the corresponding Fourier spectrum at the fluid-tank interface at $\theta = 0°$ shown in Fig. 6. The frequency of the tangential mode is found to be 0.74 Hz, which is the first tangential mode and can be identified from the wave-height history and the Fourier spectrum at the fluid-UIS interface at $\theta = 0°$ in Fig. 7. It is interesting to note that the first sloshing frequency of a rectangular tank with a fluid depth of 6.09 m (20 ft) and a tank width of 8.84 m (29 ft) (see Fig. 8) is 0.29 Hz, which is very close to that of the radial antisymmetric mode. The tank width of the rectangular tank is equivalent to the radial distance between the UIS and tank wall. Figure 9 shows the areas of the free surface which are dominated by the two sloshing modes. Apparently, when coolant sloshes, the sloshing motion in the region close to the tank wall is dominated by the radial antisymmetric mode of the radial fluid flow, whereas the sloshing response adjacent to the UIS is dominated by the tangential mode of the tangential fluid flow. The maximum wave height in the 50 s time duration is 172 cm (68.2 in.) which occurs at the fluid-tank interface at $\theta = 0°$ (see Fig. 6). The maximum wave height at fluid-UIS interface ($\theta = 0°$) is 116 cm (46 in., see Fig. 7).

In the case of the tank with off-center components, the sloshing response is dominated by four sloshing modes. They are the radial antisymmetric (0.46 Hz) and tangential (0.72 Hz) modes of the fluid which lies between the UIS and the off-center components, and the tangential (0.90 Hz) and radial antisymmetric (0.96 Hz) modes of the fluid between the off-center components and the tank. The distribution of these four modes on the free surface is shown in Fig. 10. The first two modes are similar to those of the case without off-center component as previously mentioned. The frequency of the radial antisymmetric mode, however, is increased from 0.28 Hz to 0.46 Hz. The increase of frequency is attributed to the decrease of the effective width of an equivalent rectangular tank. For the case studied, the effective width decreases from 8.84 m (the radial distance between the

UIS and the tank) to 4.87 m (the radial distance between the UIS and the off-center components). The classical fundamental sloshing frequency [4] of a rectangular tank with 6.09-m (20-ft) depth and 4.87-m (16-ft) width (see Fig. 9) is 0.40 Hz. The frequency of the tangential mode, however, is not affected by the off-center components. This is because the tangential fluid flow mainly occurs in the area adjacent to the UIS as previously mentioned. The frequency of these two modes can be identified from the time history of the wave-height plot and the corresponding Fourier spectrum of the fluid between the off-center components and the UIS. The third (0.9 Hz) and fourth (0.96 Hz) sloshing modes are caused by the fluid flowing between the off-center components and the tank wall. Again, it is interesting to know that if the distance between off-center component and tank wall, i.e., 0.93 m (36 in.), is used as the effective tank width, the classical sloshing frequency is 0.93 Hz.

The maximum wave heights at various locations for the case with off-center components are shown in Fig. 11. It is noted that the maximum wave heights shown in Fig. 11 do not occur at the same time. As indicated in Fig. 11, the maximum wave height of the case with off-center components is 101 cm (40 in.), which occurs at the off-center component and is primarily caused by the radial fluid flow between the UIS and the off-center components. The maximum wave height (40 in.) is smaller than that of the case without off-center components (68.2 in.).

The calculated fluid pressure history of fluid element 1 [at coolant-tank wall interface at $\theta = 0°$ (see Fig. 1)] for the case with off-center components is shown in Fig. 12. As can be seen, the pressure in the first 10-s period of time consists of both impulsive and convective (sloshing) pressures. After ten seconds, only the sloshing pressure remains active. The impulsive pressure vanishes because of the termination of the ground disturbance. Since the objective of this study is to find the maximum sloshing pressure acting on the submerged in-tank components, the calculation is continued to fifty seconds of time. The maximum sloshing pressure of fluid element 1 is found to be 0.0055 MPa (0.8 psi) which occurs at twenty-five seconds after the start of the ground motion or fifteen seconds after the cease of the ground motion.

The maximum sloshing pressures at tank top and midheight for the case with off-center components are shown in Fig. 13. Again, those maximum sloshing pressures do not occur at the same time. As can be seen in Fig. 13, the maximum sloshing pressure acting on the components is 0.0275 MPa (4.0 psi). The off-center components are subjected to two different types of sloshing modes, one side with a frequency of 0.46 Hz and the other side with a frequency of 0.9 Hz. Since both sloshing modes have a $\cos\theta$ distribution, it is reasonable to assume that at certain instances the sloshing pressure acting on the component will have a $\cos\theta$ distribution as shown in Fig. 14. In other words, one side of the component will be subjected to compressive loads, while the other side will be subjected to tensile loads. This is the worst loading case for a component subject to seismic sloshing. For a conservative estimate, we use the maximum sloshing pressure of 0.034 MPa (5 psi) to calculate the maximum stresses on the component. Furthermore, it is assumed that this maximum pressure is uniformly distributed along the submerged length of the component. If the component is represented by a stick model which is usually the case in the conventional component analysis, the resultant force f per unit length acting on the component (see Fig. 14) is

$$f = \int_0^{2\pi} P \cdot \cos^2\theta \, r \, d\theta , \tag{7}$$

or

$$f = \pi p r , \tag{8}$$

where p is the maximum sloshing pressure and r is the radius of the component. The total force F acting on the component is given by

$$F = f \ell , \tag{9}$$

where ℓ is the submerged length of the component plus the maximum wave height.

The bending stress at the support of a component due to the sloshing loading described above is 48.2 MPa (7 ksi), if the component is assumed to have a 3.04-m (10-ft) diameter, 2.54-cm (1-in) thickness, and 10.66-m (35 ft) long component with a submerged length of 6.09 m (20 ft). This stress should be added to other stresses for the design of reactor components.

SLOSHING RESPONSE OF A RECTANGULAR TANK WITH A COMPONENT

This section presents the results of a sloshing study performed on a rectangular tank with an internal component. The rectangular tank represents a portion of the reactor tank ($\theta = 150°$~$180°$) as shown in Fig. 1. The objectives of the study are to investigate the basic sloshing phenomena of rectangular tank with components and to compare its response with that of the cylindrical tank. For comparison purpose, the sloshing response of an identical rectangular tank with no internal component is also analyzed. The finite-element models of the rectangular tank with and without a component are shown in Fig. 15. Due to the symmetric condition, only half of the component is considered. The input motion is identical to that used in the cylindrical tank study. It is a 10-s acceleration time history having a maximum acceleration of 1 g. After ten seconds, the input motion is terminated. The seismic analysis, however, is carried out to thirty seconds.

Due to the nature of two-dimensional fluid-flow, the sloshing motion in a rectangular tank with no internal components subjected to horizontal seismic excitation is quite simple. The sloshing response is primarily dominated by the fundamental antisymmetric mode with contributions from higher modes. The first and second antisymmetric modes can be observed from the computed sloshing waves as shown in Fig. 16. The sloshing frequencies of these two modes are 0.28 Hz and 0.48 Hz, respectively. The maximum wave height in the 30-s period of time is 132 cm (52 in.), which occurs at the edge of the tank.

The free-surface wave patterns of sloshing in a rectangular tank with a component are much more complicated. A typical free-surface wave pattern is shown in Fig. 17. Basically, the presence of the component serves as a barrier which approximately divides the tank into two pools. There are two distinct antisymmetric modes. The fluid in the small pool sloshes with a frequency of 0.73 Hz (see Fig. 17), whereas the fluid in the large pool has a sloshing frequency of 0.63 Hz.

The sloshing waves at the interval of every two seconds are shown in Fig. 18. As can be seen, the free-surface waves at the narrow corner location between the component and the tank are higher than those at other locations. This is attributed to the fact that the fluid flows primarily in the direction paral-

lel to the axis of excitation. Therefore, when fluid passes the narrow path between the component and the tank, the sloshing wave height increases. The comparison of the maximum wave heights at various locations between the rectangular tank and cylindrical tank is shown in Fig. 19. The maximum wave height of the rectangular tank is 110 cm (43.2 in.) which, as mentioned before, occurs at the narrow corner location between the component and the tank. The wave height of the cylindrical tank at the same location is only 45.7 cm (18 in.). The reduction of wave height in the cylindrical tank is mainly due to the fact that fluid is allowed to flow in the circumferential direction of the tank. It is noted that the wave heights in a tank with internal components are generally smaller than those in a tank without internal components. For the cases studied here, the maximum wave height is 132 cm (52 in.) for the case without components and 110 cm (43.2 in.) for the case with components.

The maximum sloshing pressures at mid-height of the fluid for the rectangular and cylindrical tanks are shown in Fig. 20. The maximum sloshing pressure is 0.038 MPa (5.5 psi) for the rectangular tank and 0.020 MPa (3.0 psi) for the cylindrical tank. The higher pressures in the former case are attributed to the higher wave heights.

This study indicates that the flow patterns in a rectangular tank under horizontal seismic excitation are quite different from those in a cylindrical tank. The fluid in the rectangular tank mainly flows in the plane parallel to the axis of the excitation. As the fluid sloshes passing the narrow path between the component and the tank, it has to move quickly. This results in higher wave height and larger sloshing pressure at that location. For the cylindrical tank, the fluid is allowed to flow in the circumferential direction of the tank. That will reduce the wave height and thereby the sloshing pressure at the corner location between the component and the tank. As a result, the maximum wave height and pressure for the cylindrical tank occur at different locations from those of the rectangular tank.

SLOSHING RESPONSE IN THE NUCLEAR PLANT WITH SEISMIC ISOLATION

This section describes the sloshing response of a reactor tank in a nuclear plant with seismic isolation devices. The seismic isolated plant is usually designed through the use of isolators which have a very low fundamental frequency, usually below 1 Hz. The concept appears very attractive, because the low fundamental frequency of the plant is outside the frequency range of strong amplification region of the seismic motions (usually between 2 ~ 10 Hz). However, the low-frequency isolation device may cause some problems to sloshing which is also characterized by the low fundamental frequency. For this reason, a preliminary analysis of the effects of seismic isolation on sloshing response are conducted. The analysis is separated into two steps. In the first step, the seismic motion at reactor support is calculated based on a simple mathematical model which represents the reactor building by a stick and the seismic isolator by spring-damper-friction plate. In the second step, the sloshing response is calculated with a finite element model. The stick model is shown in Fig. 21 together with the isolator spring-damper-friction plate model. The pertinent data of the stick model and the seismic isolator is given in Table 1. Four cases are studied in which the reactor building is assumed to have a fundamental frequency of 1, 0.8, 0.6 (with isolator) and 3 Hz (with no isolator), respectively. A 10-s duration E-W component of El Centro acceleration time history having a maximum acceleration of 0.3 g, is applied to the base of the model. The acceleration time history at the top of the model where the reactor tank is assumed to be supported is computed using a seismic isolation computer program. This acceleration history is then used as input motion for computing the seismic response of a flexible-wall reactor tank which has a thickness of 1 in., a diameter of 70 ft, and a height of 60 ft. The fluid depth of the reactor tank is 50 ft. To simplify the study, the tank is assumed to be bottom-supported and having no internal component. The fundamental sloshing frequency is 0.25 Hz.

The computed results of the four cases studied are shown in Table 2. As can be seen, the responses (maximum relative displacement at tank-top, maximum pressures at tank-top and mid-height) of the cases with seismic isolator are significantly reduced compared to those of the case with no isolator. A reduction factor of 5 is obtained. The maximum wave height of the cases with isolator, however, is substantially increased. The increase is more pronounced when the fundamental frequency of the plant with isolator is close to that of the sloshing. For example, the maximum wave height is increased from 20.8 in. for the case of no isolator to 37.5 in. for the case of having a 0.6-Hz isolator. The wave height is increased 1.8 times even though the maximum acceleration at reactor support is decreased (see Table 2).

CONCLUSIONS

A study on the sloshing of reactor tanks subjected to horizontal seismic excitation is presented, considering the effects of internal components and seismic isolation. Emphasis is on the sloshing loads exerted on the submerged components and the effects of the components and seismic isolation on the sloshing response. The conclusions drawn from this study are:

1. The sloshing loads exerted on the submerged components could be significant. For the case studied, the maximum sloshing pressure exerted on the off-center component is 0.034 MPa (5 psi). It can produce a bending stress of the magnitude of 48.2 MPa (7 ksi) on the deck-mounted components. This additional stress should be added to other stresses obtained from the conventional component seismic analysis which does not consider sloshing loads on the components.
2. The presence of submerged components significantly change the dynamic characteristics of sloshing motion. The sloshing frequencies of the tank with off-center components are higher than those of the tank without off-center components. The sloshing wave height in tanks with off-center components are smaller. The prediction of maximum wave height based on the conventional method which does not consider the presence of off-center components is too conservative. Therefore, it should not be used in reactor designs.
3. In the rectangular tanks, the fluid mainly flows in the plane parallel to the axis of seismic excitation, whereas in the cylindrical tanks, the fluid flows in both the radial and tangential directions of the tank. The sloshing frequency of the radial fluid-flow motion can be approximately calculated from the classical solution of rectangular tank with an equivalent tank width.
4. The seismic isolator significantly reduces the seismic response of reactor tanks. How-

ever, the sloshing wave height is substantially increased. For the case studied, the wave height is increased 1.8 times, if the plant has a fundamental frequency of 0.6 Hz.

ACKNOWLEDGMENTS

The authors wish to thank Dr. S. H. Fistedis and Mr. J. Gvildys for their support during this study. This work was performed in the Engineering Mechanics Program of the Reactor Analysis and Safety Division at Argonne National Laboratory, under the auspices of the U.S. Department of Energy.

REFERENCES

1. "The Dynamic Behavior of Liquids in Moving Containers," edited by H. Norman Abramson, NASA SP-106, 1966.

2. Housner, G. W., "Dynamic Pressures on Accelerated Fluid Containers," Bulletin of the Seismological Society of America, Vol. 47, No. 1, January 1957, pp. 15-35.

3. Housner, G. W., "The Dynamic Behavior of Water Tanks," Bulletin of the Seismological Society of America, Vol. 53, No. 2, February 1963, pp. 381-387.

4. "Nuclear Reactor and Earthquake," TID 7024, prepared by Lockheed Aircraft Corporation and Holmes and Narver, Inc. for U. S. Atomic Energy Commission, August 1963, pp. 182-209 and pp. 367-390.

5. Epstein, H. I., "Seismic Design of Liquid-Storage Tanks," Journal of the Structural Division, ASCE, Vol. 102, No. ST9, September 1976, pp. 1659-1673.

6. Aslam, M., Godden, W. G., and Scalise, T., "Sloshing of Water in Annular Pressure-Suppression Pool of Boiling Water Reactor Under Earthquake Ground Motions," NUREG/CR-1083, LBL-6754, October 1979.

7. Islam, M., Godden, W. G., and Scalise, D. T., "Sloshing of Water in Torus Pressure-Suppression Pool of Boiling Water Reactors Under Earthquake Ground Motions," NUREG/CR-1082, LBL-7984.

8. Clough, R. W. and Clough, D. P., "Seismic Response of Flexible Cylindrical Tanks," paper K 5/1, 4th International Conference on Structural Mechanics in Reactor Technology, San Francisco, CA, August 1977.

9. Houser, G. W. and Haroun, M. A., "Vibration Tests of Full-Scale Liquid Storage Tanks," Proceedings of 2nd U. S. International Conference on Earthquake Engineering, Stanford University, August 1979.

10. Housner, M. A. and Housner, G. W., "Free Lateral Vibrations of Liquid Storage Tanks," Proceedings of the Third EMD Specialty Conference, Austin, TX, ASCE, September 1979, pp. 466-470.

11. Clough, D. P., "Experimental Evaluation of Seismic Design Methods for Broad Cylindrical Tanks," UCB/EERC-77/10, May 1977.

12. Niwa, A., "Seismic Behavior of Tall Liquid Storage Tanks," UCB/EERC-78-04, February 1978.

13. Manos, G. C. and Clough, R. W., "Further Study of the Earthquake Response of a Broad Cylindrical Liquid-Storage Tank Model," UCB/EERC-82/07, July 1982.

14. Liu, W. K. and [illegible], D. C., "Computer Implementation Aspects for Fluid-Structure Interaction Problems," Computer Methods in Applied Mechanics and Engineering 31, 1982, pp. 129-148.

15. Hughes, T. J. R. and Liu, W. K, "Implicit-Explicit Finite Elements in Transient Analysis," Journal of Applied Mechanics 45, 1978, pp. 371-378.

16. Ma, D. C., Gvildys, J., and Chang, Y. W., "Seismic Fluid-structure Interaction of a Large Breeder Reactor," Seismic Effects of PVP Component (ASME PVP-Vol. 88, 1984, edited by V. N. Shah and D. C. Ma.

17. Ma., D. C., et al., "Seismic Response of the Flexible Fluid-Tank System - A Numerical Study," ASME paper 82-PVP-6, ASME PVP Conference, Orlando, Florida, 1982.

18. Ma, D. C., et al., "Seismically-Induced Sloshing Phenomena in LMFBR Reactor Tanks," Advances in Containment Design and Analysis, Bd. Vol. G00214, ASME/ANS Nuclear Engineering Conference, Portland, Oregon, July 1982.

19. Ma, D. C., et al., "Seismic Behavior of Liquid-Filled Shells," Nuclear Engineering and Design, 70, 1982.

20. Ma, D. C., Gvildys, J., and Chang, Y. W., "Seismic Response of Large Suspended Tanks," ASME 83-PVP-70, ASME PVP Conference, Portland, Oregon, June 17-21, 1983.

Table 1. Pertinent Data of Stick Model

M1, M4	166 K-sec^2/ft
M2, M3	332 K - sec^2/ft
K	2.58 x 10^7 K/ft
K_{pad}	39478 K/ft (1 Hz plant frequency) 25266 K/ft (0.8 Hz plant frequency) 14212 K/ft (0.6 Hz plant frequency)
Friction coefficient	0.2
Critical damping (%)	5

Table 2. Maximum Response of Various Cases

	(1) No Isolator	(2) 1 Hz Isolator	(3) 0.8 Hz Isolator	(4) 0.6 Hz Isolator	(4)/(1)
Reactor Support					
a_{max} (g)	0.34	0.225	0.215	0.212	62%
Tank-tip					
d_{max} (in.)	0.215	0.052	0.049	0.044	20%
Tank-top					
p_{max} (psi)	4.1	1.12	1.0	0.89	22%
Tank-midheight					
p_{max} (psi)	12.4	3.0	2.9	2.6	21%
Max. Wave					
Height (in.)	20.8	25.1	27.8	37.5	180%

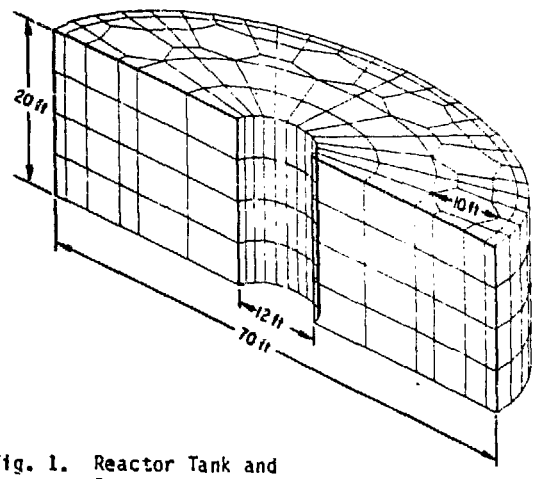

Fig. 1. Reactor Tank and Internal Components

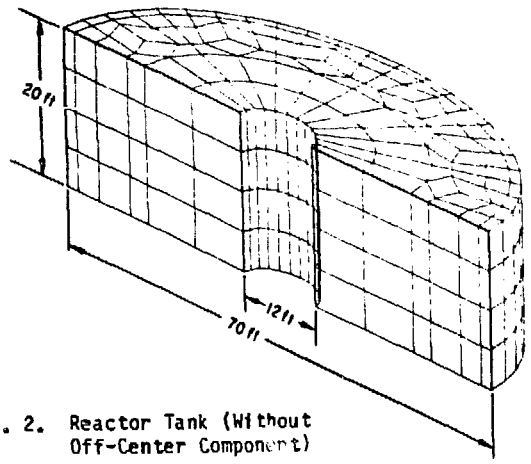

Fig. 2. Reactor Tank (Without Off-Center Component)

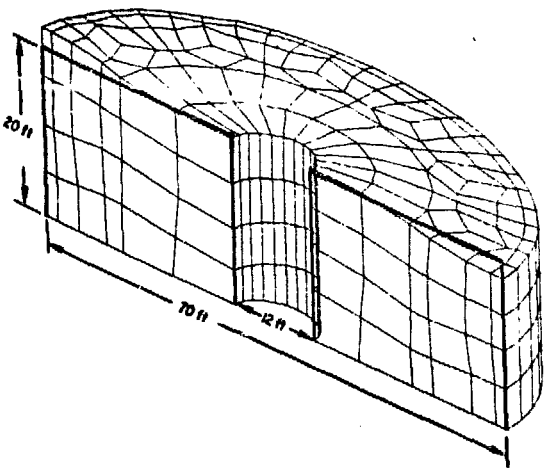

Fig. 3. Free-Surface Wave at t = 15 s (Without Off-Center Component)

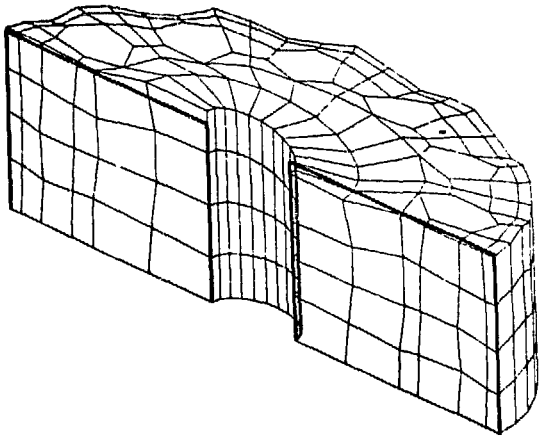

Fig. 4. Free-Surface Wave at t = 15 s (With Off-Center Component)

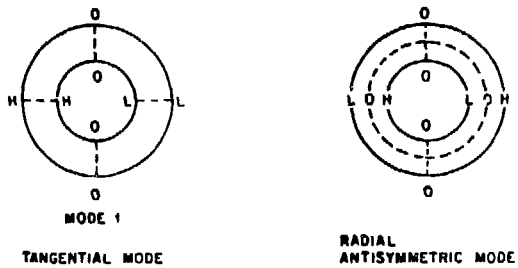

Fig. 5. First Tangential Mode and First Radial Antisymmetric Mode

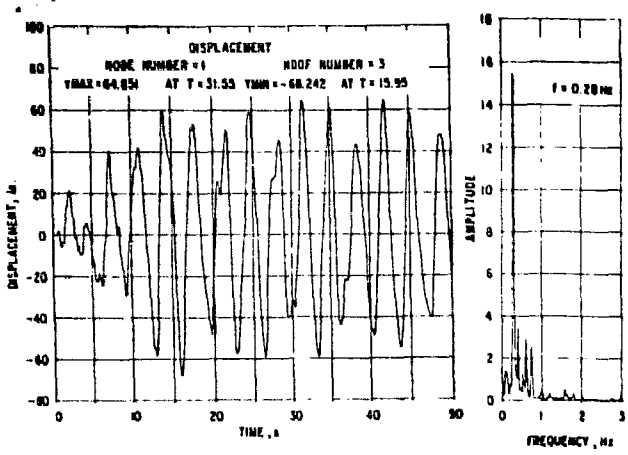

Fig. 6. Wave-Height History at Fluid-Tank Interface and Corresponding Fourier Spectrum (Without Off-Center Component)

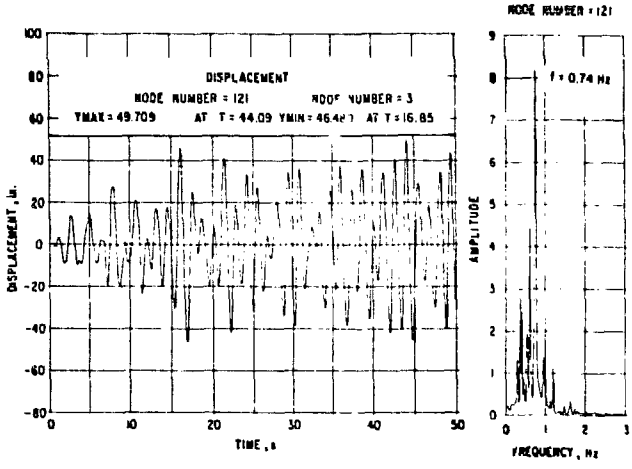

Fig. 7. Wave-Height History at Fluid-UIS Interface and Corresponding Fourier Spectrum (Without Off-Center Component)

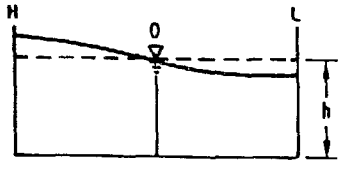

RECTANGULAR TANK

Fig. 8. First Sloshing Mode in a Rectangular Tank

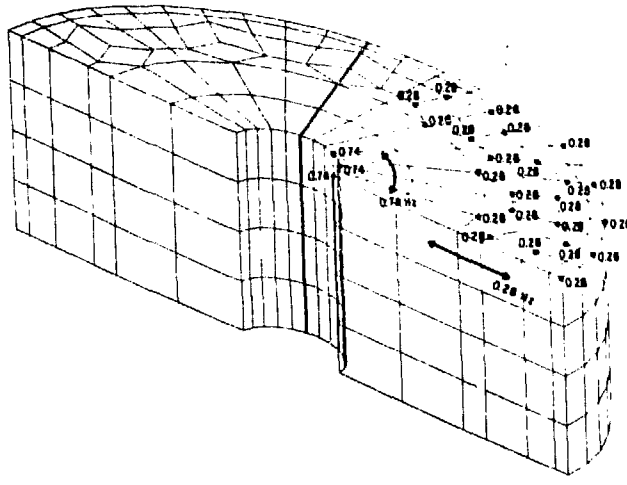

Fig. 9. Dominant Sloshing Frequency (Hz) (Without Off-Center Component)

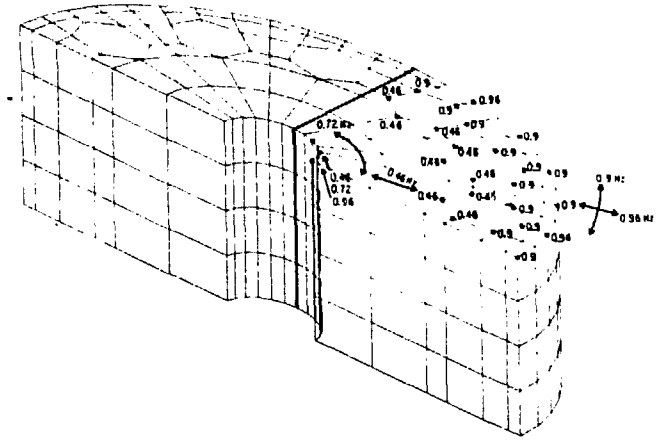

Fig. 10. Dominant Sloshing Frequency (Hz) (With Off-Center Components)

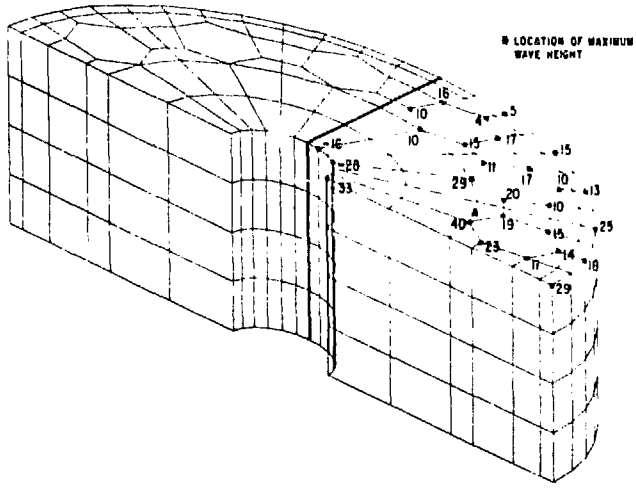

Fig. 11. Maximum Wave Heights (in.) (With Off-Center Components)

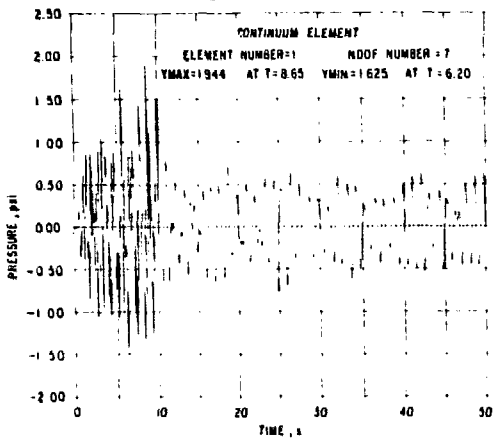

Fig. 12. Pressure History at Fluid-Tank Interface (With Off-Center Component)

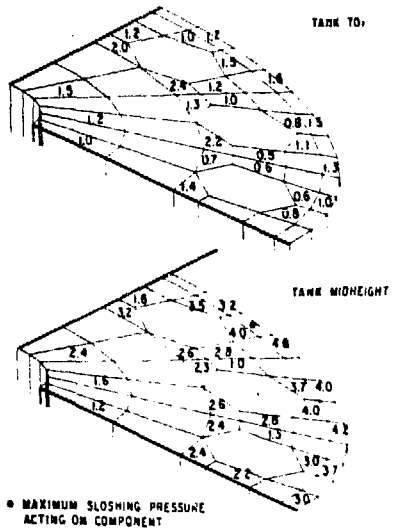

Fig. 13. Sloshing Pressure (psi) at Tank-Top and Mid-height (With Off-Center Components)

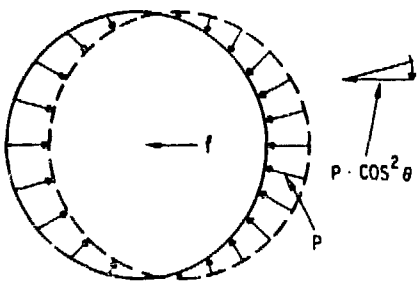

Fig. 14. Sloshing Pressure Distribution on the Component

Fig. 15. Mathematical Model of Rectangular Tank (A) With Component and (B) Without Component

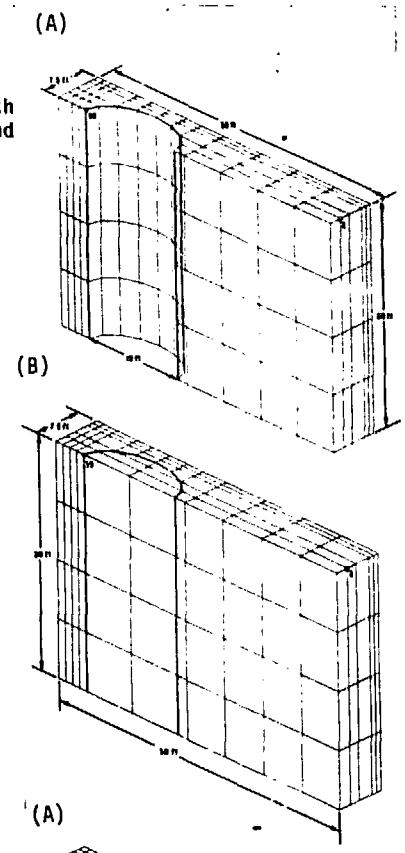

Fig. 16. (A) First Sloshing Mode and (B) Second Sloshing Mode

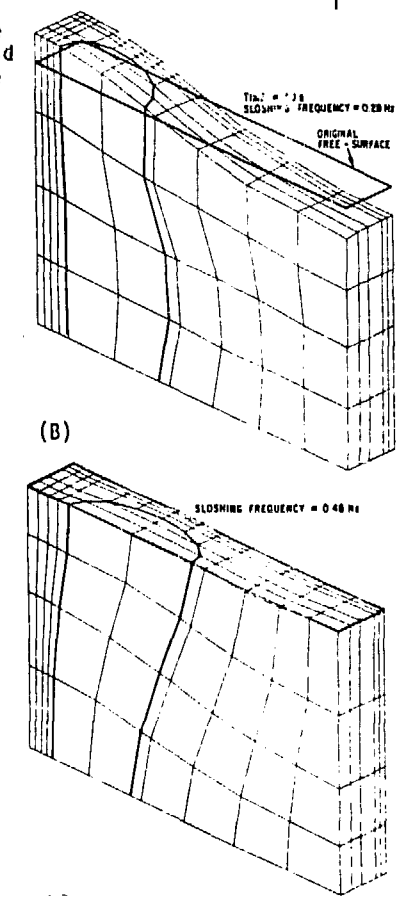

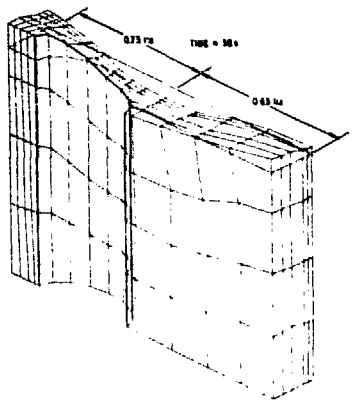

Fig. 17. Sloshing Wave Pattern at t = 30 s

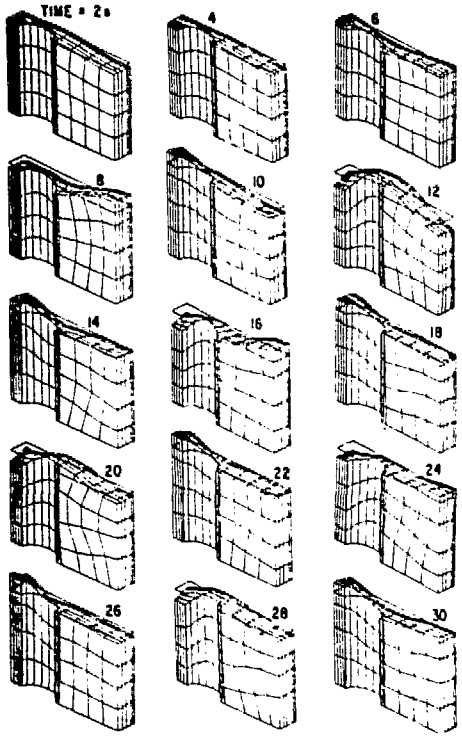

Fig. 18. Sloshing Response at Various Time

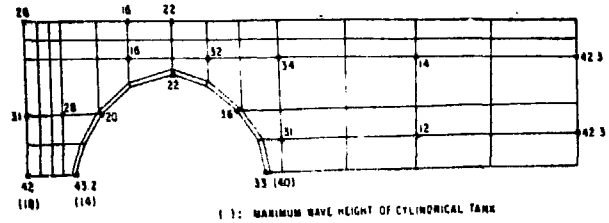

Fig. 19. Maximum Wave Heights (in.) of the Rectangular and the Cylindrical Tank With Component

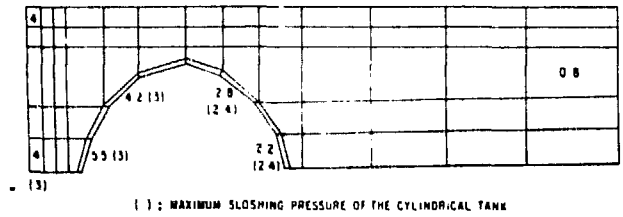

Fig. 20. Maximum Sloshing Pressures (psi) of the Rectangular and the Cylindrical Tanks With Internal Component

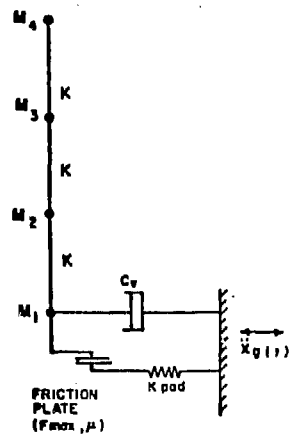

Fig. 21. Stick Model and Base Isolation